

## Research Article

# Deformation Adjustment with Single Real Signature Image for Biometric Verification Using CNN

Rakesh Kumar <sup>1</sup>, Mala Saraswat <sup>2</sup>, Danish Ather <sup>3</sup>,  
Muhammad Nasir Mumtaz Bhutta <sup>4</sup>, Shakila Basheer<sup>5</sup>, and R. N. Thakur <sup>6</sup>

<sup>1</sup>Department of Computer Engineering & Applications, GLA University Mathura, Mathura-281406, India

<sup>2</sup>Department of Computer Science and Engineering, ABES Engineering College Ghaziabad, India

<sup>3</sup>Department of Computer Science & Engineering, School of Engineering & Technology Sharda University, Grater Noida, India

<sup>4</sup>Computer Science and Information Technology (CSIT), College of Engineering, Abu Dhabi University, P.O. Box 5991, Abu Dhabi, UAE

<sup>5</sup>Department of Information Systems, College of Computer and Information Science, Princess Nourah Bint Abdulrahman University, P.O. Box 84428, Riyadh 11671, Saudi Arabia

<sup>6</sup>LBEF Campus, Kathmandu, Nepal

Correspondence should be addressed to R. N. Thakur; [rn.thakur@lbef.edu.np](mailto:rn.thakur@lbef.edu.np)

Received 29 March 2022; Revised 23 April 2022; Accepted 16 May 2022; Published 25 June 2022

Academic Editor: Shakeel Ahmad

Copyright © 2022 Rakesh Kumar et al. This is an open access article distributed under the Creative Commons Attribution License, which permits unrestricted use, distribution, and reproduction in any medium, provided the original work is properly cited.

Signature verification is the widely used biometric verification method for maintaining individual privacy. It is generally used in legal documents and in financial transactions. A vast range of research has been done so far to tackle different system issues, but there are various hot issues that remain unaddressed. The scale and orientation of the signatures are some issues to address, and the deformation of the signature within the genuine examples is the most critical for the verification system. The extent of this deformation is the basis for verifying a given sample as a genuine or forgery signature, but in the case of only a single signature sample for a class, the intra-class variation is not available for decision-making, making the task difficult. Besides this, most real-world signature verification repositories have only one genuine sample, and the verification system is abiding to verify the query signature with a single target sample. In this work, we utilize a two-phase system requiring only one target signature image to verify a query signature image. It takes care of the target signature's scaling, orientation, and spatial translation in the first phase. It creates a transformed signature image utilizing the affine transformation matrix predicted by a deep neural network. The second phase uses this transformed sample image and verifies the given sample as the target signature with the help of another deep neural network. The GPDS synthetic and MCYT datasets are used for the experimental analysis. The performance analysis of the proposed method is carried out on FAR, FRR, and AER measures. The proposed method obtained leading performance with 3.56 average error rate (AER) on GPDS synthetic, 4.15 AER on CEDAR, and 3.51 AER on MCYT-75 datasets.

## 1. Introduction

The biometric system utilizes an individual's physiological or behavioural characteristics for identification, verification, and authentication. The invariable physiological characteristics include DNA, iris, fingerprint, palm, and facial expression [1, 2], whereas behavioural traits cover voice, signature, and handwriting [1, 3, 4]. Physical characteristics such as fingerprint and iris are often used because of their

high performance. However, handwriting signatures are still being used and researched due to their ubiquitous use and cultural acceptance for personal authentication. Over centuries, its presence in legal documents, property wills and testaments, agreements, contracts, administrative records, and other legal and financial documents established it as a valuable trait. In the past, manual signature verification systems have substantially been used, but they are time-consuming and error-prone. Hence, research has been

carried out on automating the verification of handwritten signatures since the decade of 1970 [5]. It justified the research community's extensive investigation and needs industry efforts to develop better products on researched technologies.

Biometric signature systems are involved in two scenarios, namely identification and verification. In the case of signature identification, the task is to retrieve similar signature samples from a signature repository when a signature is provided as a graphical query. In comparison, the signature verification system decides whether the same signer produces a given query signature or not. Thus, the signature verification system is used to classify given handwritten signature samples as genuine or forgeries. The broad categories of forgeries are random, simple, and skilled. This categorization is based on the availability of the user's name and signature to the forger. In the first category, the forger does not have information about both the factors. Due to this reason, the forger presents a signature with a different shape and looks very different in a holistic view. In contrast, the forger knows the user's name in the category of simple forgery. Hence, the forger can produce a much similar signature compared with a genuine signature if a user uses his name or subpart of it as a signature, whereas in the case of skilled forgery, the forger possesses information about the user name and the signature. It helps the forger practice the genuine signature and produces an almost similar signature to the genuine one. Due to this reason, detecting the forged signature in the case of skilled forgery is challenging.

Depending on the signature acquisition method, signature verification systems are either online or offline [6, 7]. If the acquisition method stores the signature as a sequence of pen placement points over time, then the corresponding system is an online signature verification system. An example of such an acquisition device is digitizing tablets. Additional information is also available in digitizing tablets, such as pen's inclination and tip pressure. In contrast, the offline signature system relied on devices such as digital cameras, in which the signature is considered as an image [8]. This work is mainly focused on the offline signature verification system. The signature image has been considered a static representation of the signature for this work.

Offline signature verification can follow two different approaches namely writer-dependent and writer-independent [9]. In the writer-dependent signature verification system, a model has been trained with a genuine and forged signature for a particular writer. During inference, the model has to decide based on the similarity measure between the query signature and the genuine signature. In case, if verification is needed for a new writer, a separate model needs to get trained, which is the major drawback of writer-dependent signature verification. In comparison, the writer-independent signature verification method is a generic system and can be deployed for multiple writers. Thus, the writer-independent signature verification is more cost-efficient.

In the offline signature verification method, the feature representation is one of the most researched points by the researchers in the past [10]. For feature representation, many handcrafted features have been designed and effectively used

in the case of handwritten signature verification [9, 11–21], [5, 21–31], 71, but after the advent of deep convolutional neural networks (CNNs), the manual engineering for the features is no more needed. It can be learned by the neural network with the help of provided data [12, 32–36]. The learned features rely on the training of CNNs to learn the representation of the signature image by minimizing the loss function during the training phase. These deep learning methods have achieved good performance, but still, they are facing some trivial issues in case of signature verification.

An important issue in the training of deep neural networks is the capability of discriminating two visually close signatures, especially in the case of skilled forgery. In the case of skilled forgery, two signatures holistically look similar but only suffer from local deformation, which makes the two signatures dissimilar. It motivates us to devise a novel semi-synthetic approach to add local deformation on the signature for generating the synthetic forged version of the original image. It helps to train the network, which works efficiently to handle the most difficult case of forgery in the case of signature verification.

Another fundamental issue is the data-hungry deep learning approaches. The deep learning methods need millions of images to get trained. Ideally, in the case of signature verification, a single genuine image should be present in the repository for verification with query signature image, but in most existing methods, a set of signatures has been taken from the user (original signer) to train the deep learning method. However, to get rid of this data need for signature verification, we have mixed the signature data with the handwritten data. We consider the handwritten word as a genuine signature by a writer and the same word by another writer as a forged signature. A generic training has been conducted for the combined signature and word data. It helps to override the need for the vast amount of signature data for the training of the deep learning model for signature verification. Hence, the proposed system is writer-independent, and no separate model has been needed for a particular writer.

The rest of the study is organized into five sections. Section 2 discusses the work related to the proposed method. In Section 3, the proposed approach is described in detail. In Section 4, the experimental setup has been described. The results and analysis of the proposed work have been discussed in Section 5. The conclusions have been drawn in Section 6.

## 2. Related Work

In document analysis research, biometric authentication is referred as the unique identification of a person. This authentication can be categorized based on the behavioural and psychological traits of a person. Another categorization is soft (signature, keystrokes, voice and handwriting, gait, etc.) biometrics and hard (facial expression, fingerprint, palm print-based geometry, etc.) biometrics [37]. Soft biometrics refers to features that change frequently depending on the situation. On the other hand, hard biometrics includes most of the features that remain permanent until the particular features meet any serious accident.

Signature verification and analysis is an important soft biometric feature for person authentication, which can vary in offline and online modes. From the psychological evidence, the signature habit of an individual is a motor plan encoded thought. The moment of the motor plane at any fixed moment of time produces a common trajectory. By considering the trajectory of signature as stable regions, Parziale et al. [38] presented a stability modulated based on dynamic time wrapping (SM-DTW) for dynamic signature verification and ensured that the dynamic signature verification is more suitable to detect forgery. DTW is used to compare the string of two signatures with time.

**2.1. Online Signature Verification.** Porwik et al. [39] used the swarm intelligence technique with the probabilistic neural network (PNN) for signature verification. The dynamic feature of signature is similarity coefficients, which are selected during the Hotelling reduction process. PSO is helpful to achieve the similarity coefficients from dynamic features of signature. In the signature verification process, PNN is optimized by PSO, which is nicely tuned to the data statics of PNN classifier. Dynamic signature verification can closely represent the behavioural biometrics, which can be viewed in signing moments and speaking. For solving the problem of dynamic signature verification, Zhang [40] proposed the combination of population-based algorithms and fuzzy set theory. The evaluation of the scheme is carried out with the ATVSSLT signature verification database. The research work by the authors is referred as a measure of globally changing features and later concluded that their scheme provides a satisfactory solution for the like dynamic signature verification. Zalasinski et al. [41] also presented the dynamic signature verification based on selecting the most main partition. The key features of dynamic signature may include the change in the pressure of holding the pen and speed at particular word from the initial to middle and middle to final end of the signature. The method is primarily focused on the partition of particular parts of the signatures. Therefore, the approach increases the precision of signature processing and adapts the specific signature by removing redundant information. Dynamic methods and fuzzy set theory are used for weighted part signatures, which is a novel contribution.

**2.2. Offline Signature Verification.** Zouari et al. [42] proposed the offline signature verification on the basis of the algebraic geometry of the signature. They used partial order sets of the grids arranged in the form of lattice. Okawa [43] proposed a novel method by the fusion of the Fisher vector and KAZE features for offline signature verification. KAZE features are better to provide background information and remove the noise. The use of PCA with FV reduces the dimensionality issues and provides security by hiding the original signature. Sharif et al. [44] proposed the offline signature verification using very basic methods of feature extraction and feature processing. Initially, from the signature images binary map is prepared, which is further divided into 16 sub-blocks. By applying GA, at the individual block of signature, the received features were classified with SVM. In [45], fuzzy similarity measure and

symbolic representation techniques are used for the offline signature verification. Inter-valued symbolic data are created from LBP features of signature images and bitmap images. In general, signature duplication methods can be considered as an initiative towards the improvements in automatic signature verification. Duplicate dynamic signature generation methods include several state-of-the-art methods such as kinematic model of motor system regarding neuroscience, nonlinear distortion, and affine transformation [46]. Research on static signature duplication is limited to achieve the recent advancements in human behaviour modelling. Diaz et al. [47] firstly proposed cognitive duplication of signature behaviour algorithm to develop an offline duplicate signature generation system. During the signing process, spatial cognitive maps of human behaviour and motor system were generated with the help of linear and nonlinear transformations.

Deep convolution neural networks have immensely justified its performance in image classification, natural language processing, and several social media analytics [48]. The toughest challenge in offline signature verification is the absence of dynamic features, which can be easily helpful to catch the skill forgery. Hafemann et al. [49] presented broad literature on the problem of offline signature verification and concluded that handcrafted feature extraction methods are super shaded by deep learning. They further added better fusion of features, augmentation of datasets, and important analysis of ensemble learning and deep learning. For keeping good features that maintain the system performance, Hafemann et al. [49] proposed learning from signature images with writer-independent mode using CNN. In the experiments, the training sample and generalization samples are kept separate. Hafemann et al. [49] presented a fixed-size representation scheme for offline handwritten signature verification of different sizes. From evolution in deep learning, it is ensured that handcrafted features have been down-shaded by the features automatically extracted from the deeply stacked layers in neural network. By utilizing pyramidal pooling, Hafemann et al. [49] added fixed-size input to network layers during varied range signatures from individual users.

From the literature, it has been found that the dynamic signature verification is more efficient than offline signature verification and a widely accepted person's authentication method, but the issues with dynamic signature verification are plenty of samples required to maintain the performance. For mitigating the issues, Daiz et al. [47] proposed signature verification with only single reference. Inspired from [47], in this work, we also introduced the method, which only needs a single reference image in the offline signature verification method.

### 3. Proposed Work

The overall workflow of the proposed signature verification system is depicted in Figure 1. The system has a pre-processing phase followed by an affine alignment of given query signature images. After the affine alignment of the query image with a reference image, local features are extracted from both images. Further, the features from the reference signature are matched with their neighbourhood

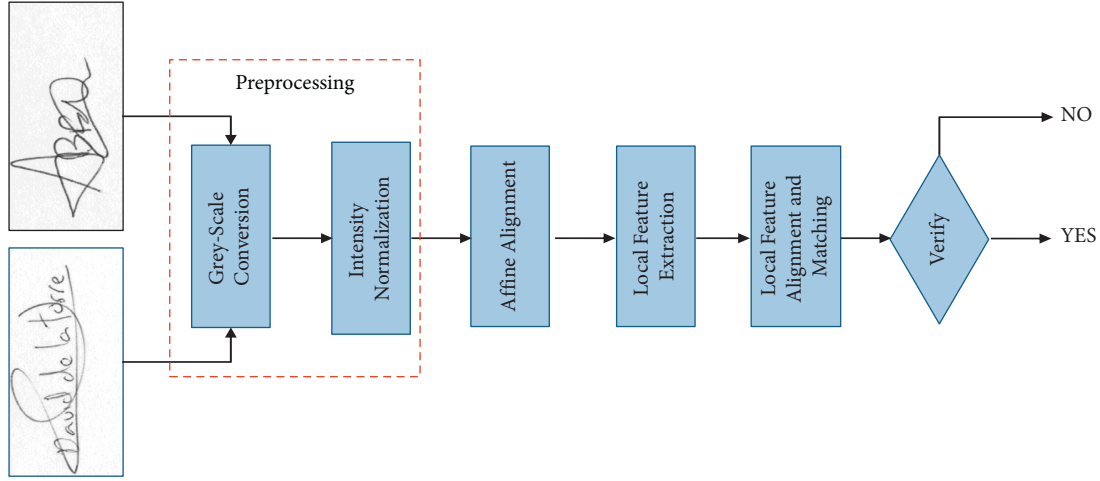


FIGURE 1: Overall workflow of proposed signature identification and verification (SIV) system.

feature in the query image and a similarity score is calculated. The signature verification decision is taken based on this similarity score.

**3.1. Conceptual Background.** The basic building block of deep learning frameworks originated from the black-box architecture of deep neural network. A brief idea of the components used for developing the deep neural network model for biometric verification system is mandatory to present in the following subsections.

**3.1.1. Convolution Neural Layer.** The deep convolutional neural network is multilayered neural network and is recently used in various challenging problems [50–52]. The neurons of a convolution layer are connected to the local section of the input data. The receptive field of a neuron is the extent of its scope in input data, and it is increased by stacking the convolution layers. The convolution operation is given as equation (1), where  $CB^k$  is the  $k^{th}$  convolution kernel weights and its bias term, respectively, and is expressing the convolution method.

$$\text{OpMap}_k = (\text{InMapCK}_k) + CB_k. \quad (1)$$

The operation of convolution is constructed by one or more combination of such kernels. All convolution layers are followed by batch normalization layer and leaky ReLU as activation function in the proposed model.

**3.1.2. Batch Normalization Layer.** The work [53, 54] revealed that deep neural networks' training is complicated and has different hyperparameters. Generally, the computational graph of a deep neural model has higher depth, leading to the convergence problem. There are some techniques [53–57] suggested to fix this issue. The batch normalization (BN) layer [56] is used in the proposed model for handling convergence problem and accelerates the network's training. In general, the BN layer is applied just before the activation layer (refer to [56] for details).

**3.1.3. Activation Function Layer.** The activation functions in a neural network work as the transfer functions. These layers transform the results of the previous layer to map it with the given ground truth. Two kinds of activation functions are the linear activation function and the nonlinear activation function. In deep neural networks, different nonlinear functions are employed as the activation. These functions are generally introduced to maintain nonlinearity concept in the network. We have adopted various classes of different activation functions as described in the following subsections.

(1) *Leaky ReLU.* It is a linear rectified function, which is in short recall as ReLU. The output of ReLU function is zero for negative input, and otherwise, input remains unchanged (refer to equation (2)). In back propagation [58], the model parameters are updated by nonnegative input values. This leads to the dying ReLU problem; therefore, the leaky ReLU activation function is applied in our network to address this issue. Here, the negative slope  $\alpha$  is not zeros but has a small value, which creates its derivative nonzeros for any input data ( $\alpha = 0.01$  in our experiments). The function corresponding to mathematical representation is given by equation (2), and its derivatives are given by equation (3). The corresponding functions are also depicted in Figure 2.

$$\text{ReLU}(z) = \max\{z, 0\}, \quad (2)$$

$$f(z) = \begin{cases} z, & z \geq 0, \\ \alpha z, & z < 0. \end{cases} \quad (3)$$

(2) *Hyperbolic Tangent Activation Function.* It is a kind of logistic sigmoid activation function, which has the important interpretation of the biological neurons. The main characteristic of hyperbolic tangent (tanh) function is having higher derivatives vanishing near zero. This is because the hyperbolic tangent function maintains its suitable property to learn the discriminative features from a higher class of varied data samples. The range of the tanh function is in the range of  $[-1, 1]$ . The tanh function and its derivatives are

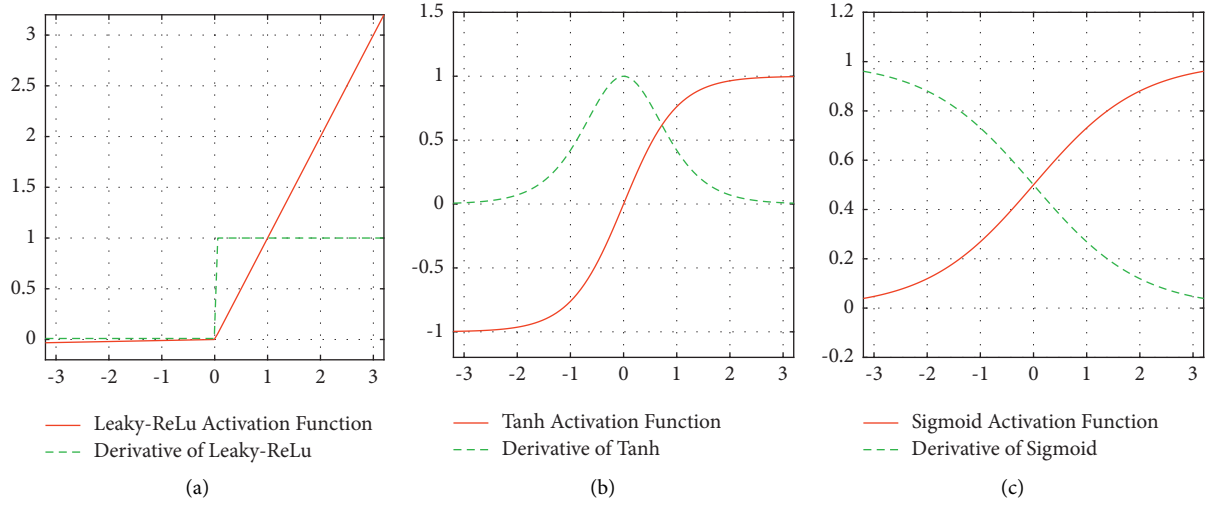


FIGURE 2: Different activation functions.

dispensed in Figure 2 and obtained by equations (4) and (5), respectively. This activation function incorporates the recurrent network units (GRU and LSTM).

$$\tanh z = \frac{e^z - e^{-z}}{e^z + e^{-z}}, \quad (4)$$

$$\tanh' z = 1 - \tanh^2 z. \quad (5)$$

(3) *Sigmoid Activation Function.* The property of sigmoid activation function yields its normalized score in the range of  $[0, 1]$  at the output scale. The mathematical expression of sigmoid function and its derivatives are explained in the figure below and calculated using equations (6) and (7), respectively. GRU and LTM unit present in recurrent network utilize the activation function for computing the corresponding activation values.

$$\sigma(z) = \frac{1}{1 + e^z}, \quad (6)$$

$$\sigma'(z) = 1 - \sigma(z). \quad (7)$$

**3.1.4. MaxPool Layer.** The MaxPool layer [59] is used to increase the receptive field of the network. This operation reduces (spatial dimensions) the size of the feature maps and decreases the computation cost. The reduction is applied only to the height and width of input data. The number of feature channels remains unchanged. It is similar to the sliding window approach with the selection of maximum element operation. The reduction in the size depends on the stride of the sliding operation. The proposed network utilizes a pooling size  $2 \times 2$  and strides  $2 \times 2$  for the pooling operation. The pooling is a nonparametric layer; therefore, there are no parameters for learning.

**3.2. Preprocessing.** A preprocessing step is not a vital phase for a convolutional neural network-based system, but it can reduce the total training time and sometimes improve the

performance of the system. Besides this, it is also instrumental in representing the input data appropriately for the subsequent phases of the system. In this work, we are incorporating greyscale conversion of colour images and their intensity normalization as preprocessing steps. After converting a colour image into a greyscale image, it is resized such that its smaller side becomes 80 pixels. Besides this, we rotated the images such that the smaller side of the image becomes its height. Finally, its intensities are normalized such that the background pixels on the image became black or near to black, and the foreground pixels (signature pixels) became white or near to white (refer to Figure 3). Here, we are not converting the signature image into black and white; instead, it is still grayscale, but the background is black as we are using it as the padding in other sections of the system.

**3.3. Affine Alignment.** To understand the importance of this phase, let us assume that we have two different signature images of the same signer and try to find out their differences. There are two types of differences between these images: (1) global difference and (2) local difference. The global difference is caused by the shift in the position of signature, size, and shape variance and the orientation of its principal axis, whereas the local difference is caused by the deformation of each pixel in the form of its position displacement and colour intensity changes (refer to Figure 4).

In this phase, the proposed system analyzes the global differences by predicting the affine transformation of query signature image with respect to reference signature image. To predict the affine transformation of query image, the proposed system utilizes two trainable neural networks: (1) CNN-1: convolution neural network and (2) FFNN-1: feed-forward neural network. The overview of this phase is depicted in Figure 4 with the CNN-1 and FFNN-1 architecture.

Here, first of all the query and reference signature image are processed with CNN-1. This network produced  $14 \times 64$ -

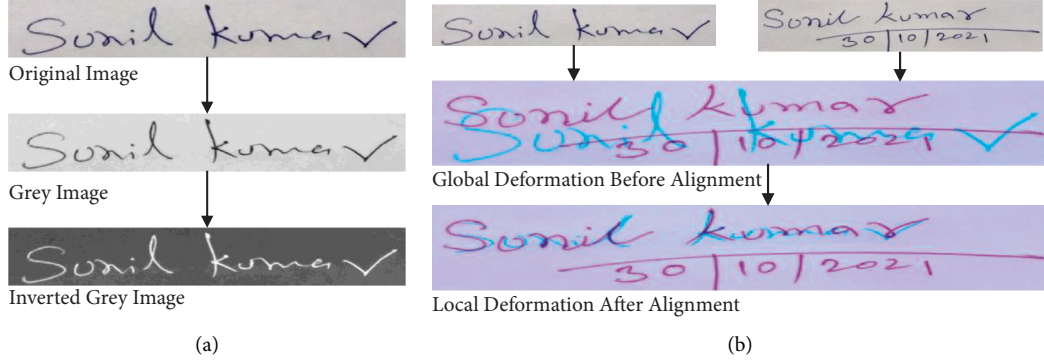


FIGURE 3: Left figure (a) shows the preprocessing steps used in the proposed system. Figure (b) in the right side is exemplifying the global deformation in pair of target signature images.

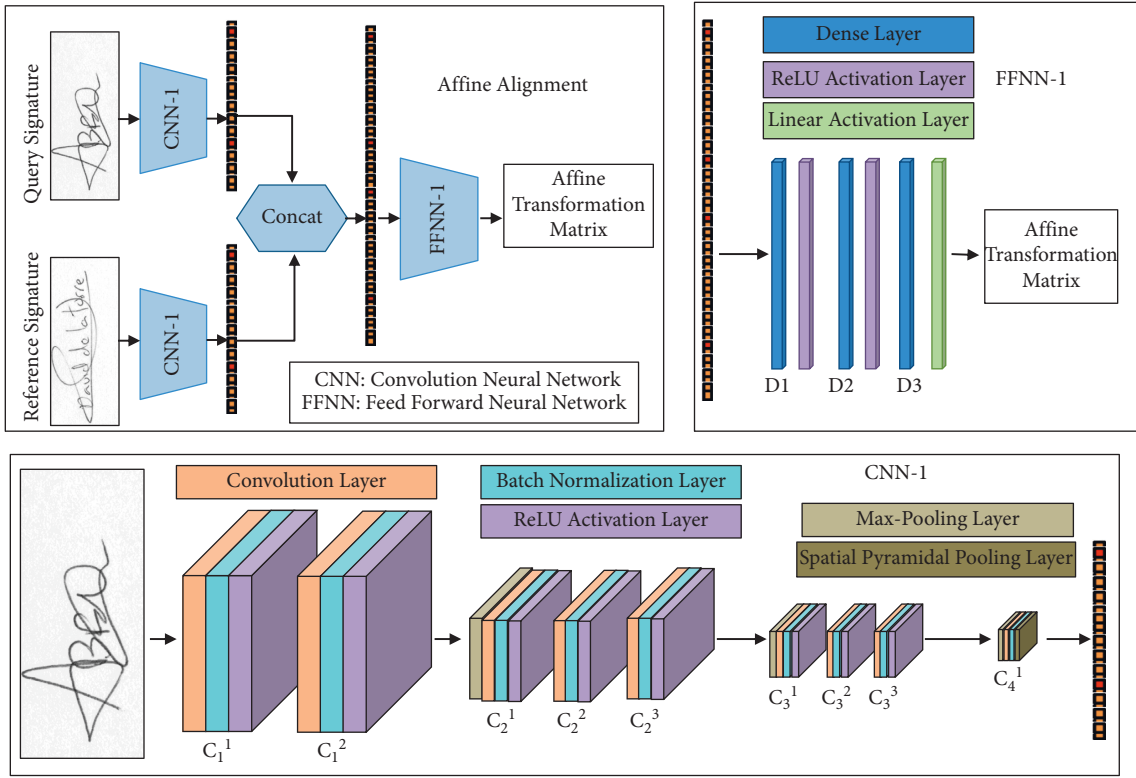


FIGURE 4: Affine alignment of query signature image with reference signature image.

dimensional vector for each image. These vectors (query image and reference image) are concatenated and passed to the FFNN-1. The FFNN-1 yields different parameters of affine transformation matrix. The architectural and parametric design detail of CNN-1 is given in Figure 4 and Table 1. Similarly, for FFNN-1 they are shown in Figure 4 and Table 2. The training procedure of this affine alignment network is explained in Subsection 3.4.

**3.4. Training of Affine Alignment Network with Semi-Synthetic Dataset.** The training of this network section is also a challenging task as we do not have labelled dataset having the affine transformation variation with ground truth. Therefore, we decided to go for a semi-synthetic dataset.

TABLE 1: Architecture description of the CNN-1: convolutional neural network-1 section of the proposed system.

Layer	#Kernel	Kernel size	#Parameter	Output size
Input	0	0	0	$H \times W \times 1$
$C_1^1$	32	$5 \times 5$	832	$H \times W \times 32$
$C_2^1$	32	$3 \times 3$	9248	$H \times W \times 32$
$C_3^1$	64	$3 \times 3$	18496	$H/2 \times W/2 \times 64$
$C_3^2$	48	$3 \times 3$	27696	$H/2 \times W/2 \times 48$
$C_3^3$	64	$3 \times 3$	27712	$H/2 \times W/2 \times 64$
$C_4^1$	128	$3 \times 3$	73856	$H/4 \times W/4 \times 128$
$C_3^1$	64	$3 \times 3$	73792	$H/4 \times W/4 \times 64$
$C_3^2$	128	$3 \times 3$	73856	$H/4 \times W/4 \times 128$
$C_4^1$	64	$3 \times 3$	73792	$H/8 \times W/8 \times 128$
Total number of parameters in CNN-1: 379280				



TABLE 2: Architecture description of the FFNN-1: feed-forward neural network-1 section of the proposed system.

Layer	#Neurons	#Parameter	Output size
Input	0	0	128
$D_t^1$	64	8256	64
$D_t^2$	128	8320	128
$D_t^3$	64	8256	64
$D_t^4$	2	130	2
$D_r^1$	64	8256	64
$D_r^2$	128	8320	128
$D_r^3$	64	8256	64
$D_r^4$	2	130	2
$D_s^1$	64	8256	64
$D_s^2$	128	8320	128
$D_s^3$	64	8256	64
$D_s^4$	2	130	2
Total number of parameters in FFNN-1: 74886			

Here, we collected signature images from all the datasets under consideration (refer to subsection 4.1) and handwritten word image samples from various datasets such as IAM [60] and CVL [61]. Considering these image samples as reference image, we applied a random affine transformation to generate query images. We utilized the random rotation with rotation angle  $\theta_{\text{rotation}} \in [-45, 45]$ , random shearing with shearing angle  $\theta_{\text{shearing}} \in [-20, 20]$ , and random scale  $S_x, S_y \in [0.5, 2.0]$  for random affine transformation (all the transformations are with respect to the center of the image). In this way, we have collected a pair of reference and query image with their corresponding transformation parameters. Utilizing this information, we have trained the affine alignment network.

A affine transformation matrix is defined by equation (8). In our case, it is the combination of different elementary transformations such as translation, scale, shear, and rotation. The transformation matrix corresponding to these elementary transformations is given by equation (9).

$$\text{AffineTransformation} = \begin{bmatrix} a_1 & b_1 & c_1 \\ a_2 & b_2 & c_2 \\ 0 & 0 & 1 \end{bmatrix}, \quad (8)$$

$$\begin{aligned} \text{Translation} &= \begin{bmatrix} 1 & 0 & t_x \\ 0 & 1 & t_y \\ 0 & 0 & 1 \end{bmatrix}, \\ \text{Scale} &= \begin{bmatrix} s_x & 0 & 0 \\ 0 & s_y & 0 \\ 0 & 0 & 1 \end{bmatrix}, \\ \text{Shear} &= \begin{bmatrix} 1 & sr_x & 0 \\ sr_y & 1 & 0 \\ 0 & 0 & 1 \end{bmatrix}, \\ \text{Rotation} &= \begin{bmatrix} \cos \theta & -\sin \theta & 0 \\ \sin \theta & \cos \theta & 0 \\ 0 & 0 & 1 \end{bmatrix}. \end{aligned} \quad (9)$$

**3.5. Local Feature Extraction and Matching.** Once the query image and reference image are aligned by transforming the reference image as affine transformation parameter (or transforming the query image as inverse affine transformation), we acquire the local features in both signature images. The local features are acquired by processing these images from the CNN-2. This network is a convolutional neural network, its architecture is depicted in Figure 5, and layered description is given in Table 3.

**3.6. Local Feature Matching.** This phase is responsible to handle the local differences in query image and reference image. The feature map (output of a CNN) generated by CNN-2 represents the neighbourhood region of size  $44 \times 44$  pixels of a cell size  $4 \times 4$  pixels. This representation is a 64-dimensional vector for each cell in feature map. Although the affine alignment phase already tackles major alignment issues, the pixel displacement can cause the local misalignment. Therefore, we calculate the Euclidean distance of a cell region in reference image with its 9 corresponding neighbours ( $3 \times 3$  window proximity) in the query image. The neighbouring cell in query image having the lowest distance is selected as the match for the corresponding cell in reference image.

**3.7. Signature Verification Decision.** This is the final step in the proposed signature verification system. Here, the matching distance of a cell in reference images is used in making a decision. It is possible that a genuine signature has some portion of signature extra or lesser with respect to reference signature (generally length of underline). So, here we need two levels of decision. First, we calculate the ratio (we call it  $DMR$ : distance matching ratio) of number of cells that have lesser matching distance than a predefined threshold ( $Th_{MD}$ ) with respect to number of cells that have it higher. We can further analyze a signature if it has  $DMR$  higher than a predefined threshold ( $Th_{DMR}$ ). The selection of  $Th_{DMR}$  depends upon the extent of extra signature that is allowed. In the proposed work, we have selected it as 4 (80% of total cell should be lower than  $Th_{MD}$ ). If a query signature gets  $DMR$  lesser than  $Th_{DMR}$  (in our case 4), then we simply discard the query signature. If the query signature passes the  $Th_{DMR}$ , then we calculate its similarity score with respect to reference signature.

The similarity score is the mean of matching distance of all cell regions, which has matching distance lesser than  $Th_{MD}$ .

## 4. Experimental Setup

**4.1. Datasets.** MYCT—this is offline signature verification dataset consisting of 75 writers. The name of the dataset is referenced from the project on science and technology under the Ministry of Spanish (Ministerio de Ciencia y Tecnología) [62]. The dataset was prepared from 15 simple signatures and 15 simulated signatures along with corresponding figure prints. The resolution of all images of signatures was maintained at 600 dpi. The dataset is useful to develop the biometric algorithms in several secured

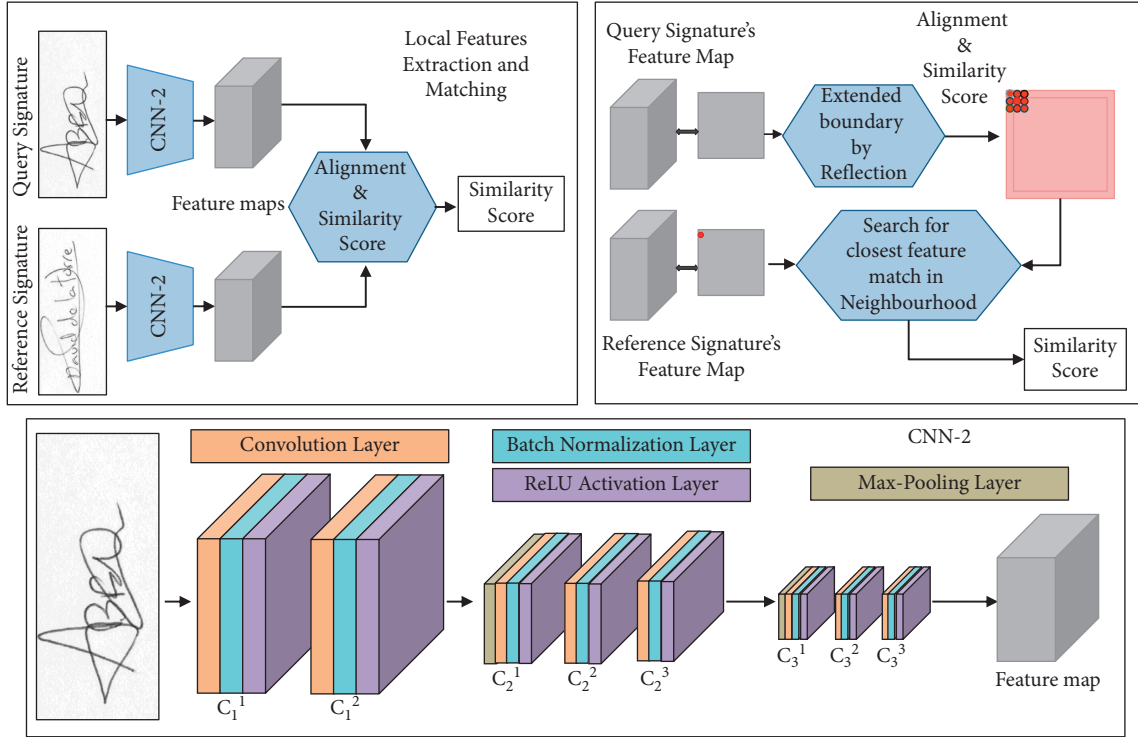


FIGURE 5: Local feature extraction and matching.

TABLE 3: Architecture description of the CNN-2:convolutional neural network-1 section of the proposed system.

Layer	#Kernel	Kernel size	#Parameter	Output size
Input	0	0	0	$H \times W \times 1$
$C_1^1$	32	$3 \times 3$	320	$H \times W \times 32$
$C_1^2$	32	$3 \times 3$	9248	$H \times W \times 32$
$C_2^1$	32	$3 \times 3$	18496	$H/2 \times W/2 \times 32$
$C_2^2$	48	$3 \times 3$	27696	$H/2 \times W/2 \times 48$
$C_2^3$	32	$3 \times 3$	27712	$H/2 \times W/2 \times 32$
$C_3^1$	64	$3 \times 3$	73856	$H/4 \times W/4 \times 64$
$C_3^2$	48	$3 \times 3$	73792	$H/4 \times W/4 \times 48$
$C_3^3$	64	$3 \times 3$	36928	$H/4 \times W/4 \times 64$
Total number of parameters in CNN-2: <b>268048</b>				

TABLE 4: Comparison of the proposed system with other (including current state-of-the-art) methods with MCYT-75 dataset.

Author	Verification type	No. of training sample	FRR	FAR	AER
[4]	WD	5G	32.4	26.84	—
		10G	22.93	22.04	—
[65]	—	5G	6.67	12.44	9.56
[66]	WD	10G	23.25	4.53	—
		10G	12.61	7.53	—
[42]	WD	5G	4.48	25.19	5.62
		10G	4.96	17.21	3.45
[67]	WD	10G	12.53	13.16	—
		5G	15.47	13.42	—
		5G	6.67	6.67	6.67
[44]	WD	10G	6.25	5.67	5.96
		12G	3.67	6.67	5.0
		5G	4.12	4.48	4.30
Ours	WI	10G	3.68	3.96	3.82
		12G	3.49	3.53	3.51

TABLE 5: Comparison of the proposed system with other (including current state-of-the-art) methods with CEDAR dataset.

Author	Verification type	No. of training sample	FRR	FAR	AER
[68]	WI	24G	—	—	8.33
[69]	WD	16G	6.36	5.68	6.02
[33]	WD	12G	9.36	7.84	8.60
[42]	WD	5G	4.44	15.91	3.64
		10G	5.83	11.52	2.74
		4G	—	—	8.70
[70]	WI	8G	7.41	8.25	7.83
		12G	—	—	5.60
		5G	12.5	8.33	10.41
[44]	WD	10G	8.33	4.17	6.25
		12G	4.67	4.67	4.67
		5G	4.32	7.84	6.08
Ours	WI	10G	5.72	4.12	5.92
		12G	3.97	4.33	4.15

domains. GPDS—this is an offline signature verification database developed in signal processing laboratory (Grupo de Procesado Digital de la señal) GPDS at University of Las Palmas de Gran Canaria, Spain [63]. GPDS consists of 24 genuine signatures and 30 forgery signatures from each of 960 individuals. The signatures are black and white format with 300 dpi. During the collection of samples, two different sizes of boxes are chosen, one is 5 cm by 1.8 cm and another is 4.5 cm by 2.5 cm. CEDAR—this is an online handwritten text database consisting of the samples of handwritten text of tablet and line of text collected from 200 writers [64]. CEDAR signature recognition dataset was developed at Buffalo University. The dataset consists of 24 samples for



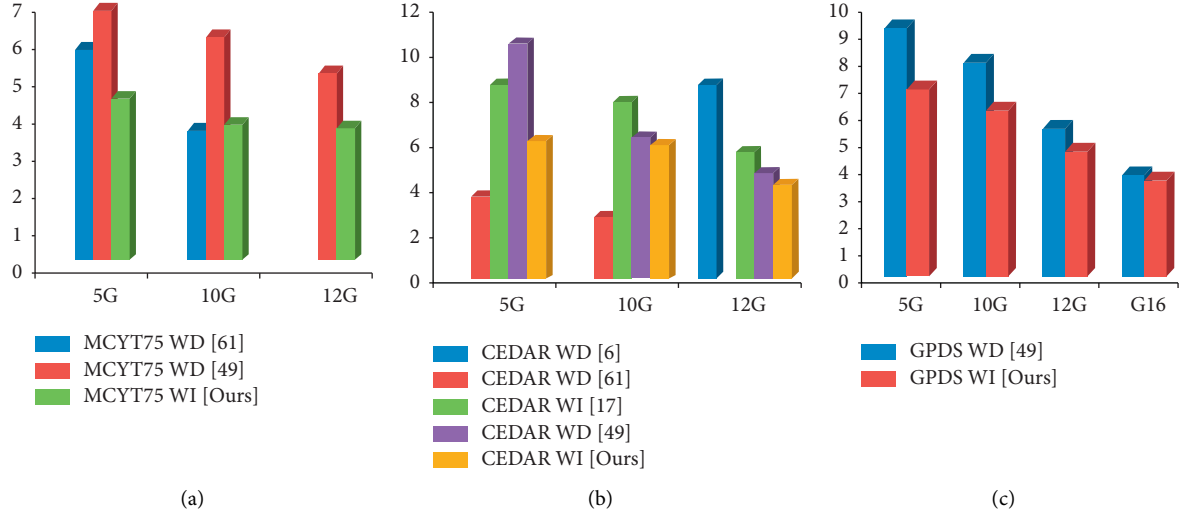


FIGURE 6: Comparison of AER on MYCT-75 (a) CEDAR (b) and GPDS (c) datasets along with different sizes of data samples.

each genuine and simulated signature from 55 enrolled forgeries. The simulated signatures include both simple and forgeries. The dataset is very large as it contains 105,573 numbers of words.

**4.2. Evaluation Criteria.** The results obtained from the proposed work are compared with current state-of-the-art methods on different standard datasets and with different evaluation criteria. We have tested the performance of the system through writer-independent signature verification task considering all reference signatures as a separate entity. We are listing the performance of the proposed system with three evaluation measures such as (1) FRR, (2) FAR, and (3) AER.

**4.2.1. FRR.** It stands for false rejection rate, a very important evaluation parameter in the biometric system to measure the likelihood that the biometric-based security system incorrectly rejects the access attempt made by the authentic user of the system. Mathematically (equation (10)), FRR is calculated as a ratio of the total counts of false rejections and total identification attempts.

$$FRR = \frac{FN}{TP + FN} \quad (10)$$

**4.2.2. FAR.** False acceptance rate or FAR is also a likelihood measure to determine that the biometric system incorrectly accepts the access attempt by the unauthentic user. In terms of mathematical formula, FAR (equation (11)) of a biometric system is the ratio of total counts of false acceptances and total number of identification attempts.

$$FAR = \frac{FP}{FP + TN} \quad (11)$$

**4.2.3. AER.** The average error rate or AER is termed as the best threshold value at which the curve of FAR and FRR meets at a point. It generally determines the stability of the system. It is mathematically computed as an average of FRR and FAR as follows:

$$AER = \frac{FAR + FRR}{2} \quad (12)$$

## 5. Results and Analysis

The proposed system has been extensively validated on the three public datasets of signature verification, namely MCYT-75, CEDAR, and GPDS. The proposed method is also compared with other state-of-the-art methods. The evaluation results for the MCYT-75 dataset are summarized in Table 4. From Table 4, it has been observed that for the 5G and 12G training samples, our proposed method has reported the least average error rate. The proposed system has achieved the least false acceptance rate (FAR) and false reject rate for 5G, 10G, and 12G training samples. This shows the proposed approach's robustness compared with other state-of-the-art methods for the MCYT-75 dataset.

For the CEDAR dataset, the quantitative results, along with the state-of-the-art approaches, are mentioned in Table 5. From Table 5, it has been found that for independent writer setting, our method is best performing as compared to the other 12G training samples. Even the proposed method has achieved the least average error rate for 12G compared with all methods (writer-independent and writer-dependent). The proposed system also achieves least false rejection rate and false acceptance rate for all settings of training samples. Figure 6 presents the average error rate (AER) for different samples taken from all three mentioned datasets. It also presents the comparative results against the mentioned state of the art. Another set of comparisons is shown in Figure 7 against the different training samples of independent and dependent writers with their rate of performance.

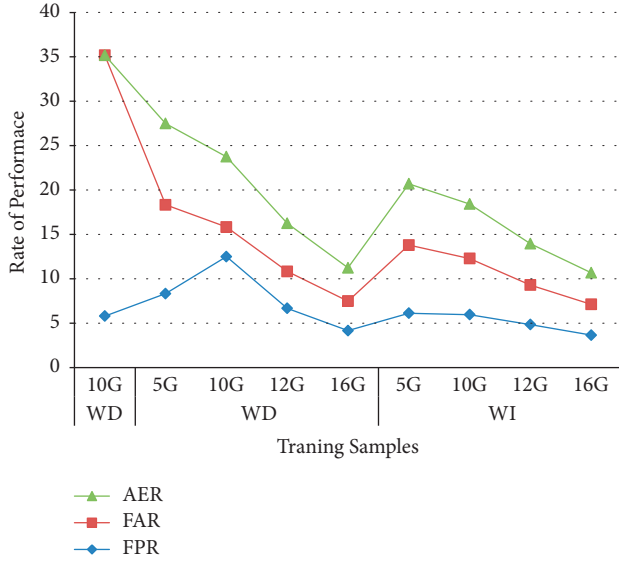


FIGURE 7: Overall comparative performance in terms of FRR, FAR, and AER on MYCT-75, GPDS, and CEDAR datasets.

TABLE 6: Comparison of the proposed system with other (including current state-of-the-art) methods with GPDS synthetic dataset.

Author	Verification type	No. of training sample	FRR	FAR	AER
[67]	WD	10G	5.80	29.49	—
		5G	8.33	10	9.16
[44]	WD	10G	12.5	3.33	7.92
		12G	6.67	4.16	5.42
		16G	4.16	3.33	3.75
		5G	6.12	7.68	6.90
Ours	WI	10G	5.96	6.32	6.14
		12G	4.84	4.46	4.65
		16G	3.65	3.47	3.56

The impact of the proposed method for the GPDS synthetic dataset is summarized in Table 6. The proposed method has achieved the best results on the AER metric for all training sample settings. The proposed method has also outperformed [44] on the metric of false rejection rate. From Tables 4–6, it is observed that the robustness of the proposed approach is compared with other existing approaches and has been validated with satisfactory measures.

## 6. Conclusion

Generally, signatures are composed of multiple components, and most of them do not provide the necessary information. For example, the date and curved line used below the signature must be ignored since it does not add any information for writer identification. Alternatively, this may help to remove the processing overheads. Interpersonal similarity and high intrapersonal variability are the challenging factors for achieving satisfactory performance to generalize offline signature verification. This may be supposed to extract the most discriminant and stable feature sets from the wide variety of geographical-invariant signers. In this study, we

presented a practical verification problem against the forgeries. In the context of feature extraction for writer-independent signature verification, the line-up future directions may be planned to fuse nonhandcrafted features. In the case of adversarial machine learning in the security domain, an interesting future direction can be added to analyze the impact of sharp physical attacks by printing the adversarial noise over the signatures. According to the writer's perspective, another future line can be encouraged to develop a better deep network than the Siamese network and the loss functions to introduce versatile reference signatures. Signature localization is also an important domain that can assist in signature verification in an image.

## Data Availability

The data used to support the study are cited within the article and are publicly available.

## Conflicts of Interest

The authors declared no conflicts of interest.

## Acknowledgments

This research was supported by Princess Nourah Bint Abdulrahman University Researchers Supporting Project, number (PNURSP2022R195), Princess Nourah Bint Abdulrahman University, Riyadh, Saudi Arabia.

## References

- [1] N. Kumar and A. Sharma, "A spoofing security approach for facial biometric data authentication in unconstrained environment," in *Progress in Advanced Computing and Intelligent Engineering*, pp. 437–448, Springer, Singapore, 2019.
- [2] J.-C. Lee, "A novel biometric system based on palm vein image," *Pattern Recognition Letters*, vol. 33, no. 12, pp. 1520–1528, 2012.
- [3] M. Sharif, S. Anis, M. Raza, and S. Mohsin, "Enhanced svd based face recognition," *Journal of Applied Computer Science Methods*, vol. 6, no. 12, 2012.
- [4] M. Sharif, S. Mohsin, M. Y. Javed, and M. A. Ali, "Single image face recognition using laplacian of Gaussian and discrete cosine transforms," *The International Arab Journal of Information Technology*, vol. 9, no. 6, pp. 562–570, 2012.
- [5] D. Rivard, E. Granger, and R. Sabourin, "Multi-feature extraction and selection in writer-independent off-line signature verification," *International Journal on Document Analysis and Recognition*, vol. 16, no. 1, pp. 83–103, 2013.
- [6] E. Parcham, M. Ilbeygi, and M. Amini, "Cbapsnet: A novel writer-independent offline signature verification model using a cnn-based architecture and capsule neural networks," *Expert Systems with Applications*, vol. 185, Article ID 115649, 2021.
- [7] R. Plamondon and S. N. Srihari, "Online and off-line handwriting recognition: a comprehensive survey," *IEEE Transactions on Pattern Analysis and Machine Intelligence*, vol. 22, no. 1, pp. 63–84, 2000.
- [8] D. Impedovo and G. Pirlo, "Automatic signature verification: The state of the art," *IEEE Transactions on Systems, Man, and Cybernetics, Part C (Applications and Reviews)*, vol. 38, no. 5, pp. 609–635, 2008.

- [9] D. Bertolini, L. S. Oliveira, E. Justino, and R. Sabourin, "Reducing forgeries in writer-independent off-line signature verification through ensemble of classifiers," *Pattern Recognition*, vol. 43, no. 1, pp. 387–396, 2010.
- [10] L. G. Hafemann, R. Sabourin, and L. S. Oliveira, "Offline handwritten signature verification - Literature review," in *Proceedings of the 2017 Seventh International Conference on Image Processing Theory, Tools and Applications (IPTA)*, pp. 1–8, IEEE, Montreal, QC, Canada, December 2017.
- [11] H. Baltzakis and N. Papamarkos, "A new signature verification technique based on a two-stage neural network classifier," *Engineering Applications of Artificial Intelligence*, vol. 14, no. 1, pp. 95–103, 2001.
- [12] J. Coetzer, "Off-line signature verification," *PhD Thesis*, University of Stellenbosch, Stellenbosch, 2005.
- [13] P. S. Deng, H.-Y. M. Liao, C. W. Ho, and H.-R. Tyan, "Wavelet-based off-line handwritten signature verification," *Computer Vision and Image Understanding*, vol. 76, no. 3, pp. 173–190, 1999.
- [14] J.-P. Drouhard, R. Sabourin, and M. Godbout, "A neural network approach to off-line signature verification using directional pdf," *Pattern Recognition*, vol. 29, no. 3, pp. 415–424, 1996.
- [15] A. El-Yacoubi, E. J. R. Justino, R. Sabourin, and F. Bortolozzi, "Off-line signature verification using hmms and cross-validation," in *Proceedings of the Neural Networks for Signal Processing X. Proceedings of the 2000 IEEE Signal Processing Society Workshop (Cat. No. 00TH8501)*, pp. 859–868, IEEE, Sydney, NSW, Australia, December 2000.
- [16] G. S. Eskander, R. Sabourin, and E. Granger, "Hybrid writer-independent-writer-dependent offline signature verification system," *IET Biometrics*, vol. 2, no. 4, pp. 169–181, 2013.
- [17] J. Hu and Y. Chen, "Offline signature verification using real adaboost classifier combination of pseudo-dynamic features," in *Proceedings of the 2013 12th International Conference on Document Analysis and Recognition*, pp. 1345–1349, IEEE, Washington DC, August 2013.
- [18] E. J. Justino, A. El Yacoubi, F. Bortolozzi, and R. Sabourin, "An off-line signature verification system using hmm and graphometric features," in *Proceedings of the 4th International Workshop on Document Analysis Systems*, pp. 211–222, Citeseer, France, 2000.
- [19] M. I. Malik, M. Liwicki, A. Dengel, S. Uchida, and V. Frinken, "Automatic signature stability analysis and verification using local features," in *Proceedings of the 2014 14th International Conference on Frontiers in Handwriting Recognition*, pp. 621–626, IEEE, Hersionissos, Greece, September 2014.
- [20] W. F. Nemcek and W. C. Lin, "Experimental investigation of automatic signature verification," *IEEE Transactions on Systems, Man, and Cybernetics*, vol. SMC-4, no. 1, pp. 121–126, 1974.
- [21] L. S. Oliveira, E. Justino, C. Freitas, and R. Sabourin, "The graphology applied to signature verification," in *Proceedings of the 12th Conference of the International Graphonomics Society*, pp. 286–290, Italy, 2005.
- [22] M. R. Pourshahabi, M. H. Sigari, and H. R. Pourreza, "Offline handwritten signature identification and verification using contourlet transform," in *Proceedings of the 2009 International Conference of Soft Computing and Pattern Recognition*, pp. 670–673, IEEE, Malacca, Malaysia, December 2009.
- [23] R. Sabourin and J.-P. Drouhard, "Off-line signature verification using directional pdf and neural networks," in *Proceedings of the 11th IAPR International Conference on Pattern Recognition. Vol. II. Conference B: Pattern Recognition Methodology and Systems*, pp. 321–325, IEEE, The Hague, Netherlands, September 1992.
- [24] R. Sabourin and G. Genest, "An extended-shadow-code based approach for off-line signature verification. i. evaluation of the bar mask definition," in *Proceedings of the 12th IAPR International Conference on Pattern Recognition, Vol. 3-Conference C: Signal Processing (Cat. No. 94CH3440-5)*, pp. 450–453, IEEE, Jerusalem, Israel, October 1994.
- [25] Y. Serdouk, H. Nemmour, and Y. Chibani, "Combination of oc-lbp and longest run features for off-line signature verification," in *Proceedings of the 2014 Tenth International Conference on Signal-Image Technology and Internet-Based Systems*, pp. 84–88, IEEE, Marrakech, Morocco, November 2014.
- [26] J. Ruiz-del-Solar, C. Devia, P. Loncomilla, and F. Concha, "Offline signature verification using local interest points and descriptors," in *Iberoamerican Congress on Pattern Recognition*, pp. 22–29, Springer, Berlin, Heidelberg, 2008.
- [27] J. F. Vargas, C. M. Travieso, J. B. Alonso, and M. A. Ferrer, "Off-line signature verification based on gray level information using wavelet transform and texture features," in *Proceedings of the 2010 12th International Conference on Frontiers in Handwriting Recognition*, pp. 587–592, IEEE, Kolkata, India, November 2010.
- [28] J. F. Vargas, M. A. Ferrer, C. M. Travieso, and J. B. Alonso, "Off-line signature verification based on grey level information using texture features," *Pattern Recognition*, vol. 44, no. 2, pp. 375–385, 2011.
- [29] M. B. Yilmaz, B. Yanikoglu, C. Tirkaz, and A. Kholmatov, "Offline signature verification using classifier combination of hog and lbp features," in *Proceedings of the 2011 International Joint Conference on Biometrics (IJCB)*, pp. 1–7, IEEE, Washington, DC, USA, October 2011.
- [30] M. Zalasinski and K. Cpalka, "A new method for signature verification based on selection of the most important partitions of the dynamic signature," *Neurocomputing*, vol. 289, pp. 13–22, 2018.
- [31] E. N. Zois, L. Alewijnse, and G. Economou, "Offline signature verification and quality characterization using poset-oriented grid features," *Pattern Recognition*, vol. 54, pp. 162–177, 2016.
- [32] S. Basheer, S. Bhatia, and S. B. Sakri, "Computational modeling of dementia prediction using deep neural network: Analysis on oasis dataset," *IEEE Access*, vol. 9, pp. 42449–42462, 2021.
- [33] R. K. Bharathi and B. H. Shekar, "Off-line signature verification based on chain code histogram and support vector machine," in *Proceedings of the 2013 International Conference on Advances in Computing, Communications and Informatics (ICACCI)*, pp. 2063–2068, IEEE, Mysore, India, August 2013.
- [34] A. S. Britto Jr, R. Sabourin, and L. E. S. Oliveira, "Dynamic selection of classifiers-A comprehensive review," *Pattern Recognition*, vol. 47, no. 11, pp. 3665–3680, 2014.
- [35] S. Siyuan Chen and S. Srihari, "A new off-line signature verification method based on graph," in *Proceedings of the 18th International Conference on Pattern Recognition (ICPR'06)*, pp. 869–872, IEEE, Hong Kong, August 2006.
- [36] N. Kumar, "Human activity recognition from histogram of spatiotemporal depth features," *International Journal of Computational Intelligence Studies*, vol. 8, no. 4, pp. 309–329, 2019.
- [37] S. Barzut, M. Milosavljević, S. Adamović, M. Saračević, N. Maček, and M. Gnjatović, "A novel fingerprint biometric cryptosystem based on convolutional neural networks," *Mathematics*, vol. 9, no. 7, p. 730, 2021.

- [38] A. Parziale, M. Diaz, M. A. Ferrer, and A. Marcelli, "Sm-dtw: Stability modulated dynamic time warping for signature verification," *Pattern Recognition Letters*, vol. 121, pp. 113–122, 2019.
- [39] P. Porwik, R. Doroz, and T. Orczyk, "Signatures verification based on pnn classifier optimised by pso algorithm," *Pattern Recognition*, vol. 60, pp. 998–1014, 2016.
- [40] B. Zhang, "Off-line signature verification and identification by pyramid histogram of oriented gradients," *International Journal of Intelligent Computing and Cybernetics*, vol. 3, no. 4, pp. 611–630, 2010.
- [41] M. Zalaśiński, K. Łapa, and K. Cpałka, "Prediction of values of the dynamic signature features," *Expert Systems with Applications*, vol. 104, pp. 86–96, 2018.
- [42] R. Zouari, R. Mokni, and M. Kherallah, "Identification and verification system of offline handwritten signature using fractal approach," in *Proceedings of the International Image Processing, Applications and Systems Conference*, pp. 1–4, IEEE, Sfax, Tunisia, November 2014.
- [43] M. Okawa, "Synergy of foreground-background images for feature extraction: Offline signature verification using Fisher vector with fused KAZE features," *Pattern Recognition*, vol. 79, pp. 480–489, 2018.
- [44] M. Sharif, M. A. Khan, M. Faisal, M. Yasmin, and S. L. Fernandes, "A framework for offline signature verification system: Best features selection approach," *Pattern Recognition Letters*, vol. 139, pp. 50–59, 2018.
- [45] A. Alaei, S. Pal, U. Pal, and M. Blumenstein, "An efficient signature verification method based on an interval symbolic representation and a fuzzy similarity measure," *IEEE Transactions on Information Forensics and Security*, vol. 12, no. 10, pp. 2360–2372, 2017.
- [46] P. Bhowal, D. Banerjee, S. Malakar, and R. Sarkar, "A two-tier ensemble approach for writer dependent online signature verification," *Journal of Ambient Intelligence and Humanized Computing*, vol. 13, no. 1, pp. 21–40, 2022.
- [47] M. Diaz, A. Fischer, M. A. Ferrer, and R. Plamondon, "Dynamic signature verification system based on one real signature," *IEEE Transactions on Cybernetics*, vol. 48, no. 1, pp. 228–239, 2016.
- [48] K. Chakraborty, S. Bhatia, S. Bhattacharyya, J. Platos, R. Bag, and A. E. Hassanien, "Sentiment Analysis of COVID-19 tweets by Deep Learning Classifiers-A study to show how popularity is affecting accuracy in social media," *Applied Soft Computing*, vol. 97, Article ID 106754, 2020.
- [49] L. G. Hafemann, R. Sabourin, and L. S. Oliveira, "Learning features for offline handwritten signature verification using deep convolutional neural networks," *Pattern Recognition*, vol. 70, pp. 163–176, 2017.
- [50] K. Dev, S. A. Khowaja, A. S. Bist, V. Saini, and S. Bhatia, "Triage of potential covid-19 patients from chest x-ray images using hierarchical convolutional networks," *Neural Computing & Applications*, vol. 25, pp. 1–16, 2021.
- [51] Y. LeCun, L. Bottou, Y. Bengio, and P. Haffner, "Gradient-based learning applied to document recognition," *Proceedings of the IEEE*, vol. 86, no. 11, pp. 2278–2324, 1998.
- [52] Y. LeCun, K. Kavukcuoglu, and C. Farabet, "Convolutional networks and applications in vision," in *Proceedings of the 2010 IEEE International Symposium on Circuits and Systems*, pp. 253–256, Paris, France, June 2010.
- [53] X. Glorot and Y. Bengio, "Understanding the difficulty of training deep feedforward neural networks," in *Proceedings of the thirteenth international conference on artificial intelligence and statistics*, pp. 249–256, Sardinia, Italy, 2010.
- [54] K. He, X. Zhang, S. Ren, and J. Sun, "Delving deep into rectifiers: surpassing human-level performance on imagenet classification," in *Proceedings of the IEEE international conference on computer vision*, pp. 1026–1034, Santiago, Chile, December 2015.
- [55] I. Goodfellow, J. Pouget-Abadie, M. Mirza et al., "Generative adversarial nets," in *Advances in Neural Information Processing Systems*, pp. 2672–2680, 2014.
- [56] S. Ioffe and C. Szegedy, "Batch normalization: accelerating deep network training by reducing internal covariate shift," arXiv:1502.03167, 2015.
- [57] N. Srivastava, G. Hinton, A. Krizhevsky, I. Sutskever, and R. Salakhutdinov, "Dropout: a simple way to prevent neural networks from overfitting," *Journal of Machine Learning Research*, vol. 15, no. 1, pp. 1929–1958, Washington, D.C, USA, 2014.
- [58] R. Hecht-Nielsen, "Theory of the Backpropagation Neural Network," in *Proceedings of the International Joint Conference on Neural Networks*, pp. 593–611, IEEE, June 1989.
- [59] A. Krizhevsky, I. Sutskever, and G. E. Hinton, "Imagenet classification with deep convolutional neural networks," *Advances in Neural Information Processing Systems*, vol. 25, 2012.
- [60] U.-V. Marti and H. Bunke, "The iam-database: an english sentence database for offline handwriting recognition," *International Journal on Document Analysis and Recognition*, vol. 5, no. 1, pp. 39–46, 2002.
- [61] F. Kleber, S. Fiel, M. Diem, and R. Sablatnig, "Cvl-database: An off-line database for writer retrieval, writer identification and word spotting," in *Proceedings of the Document Analysis and Recognition (ICDAR)*, pp. 560–564, IEEE, Washington, DC, USA, August 2013.
- [62] J. Ortega-Garcia, J. Fierrez-Aguilar, D. Simon et al., "Mcyt baseline corpus: a bimodal biometric database," *IEE Proceedings - Vision, Image and Signal Processing*, vol. 150, no. 6, pp. 395–401, 2003.
- [63] F. Vargas, M. Ferrer, C. Travieso, and J. Alonso, "Off-line handwritten signature gpdfs-960 corpus," in *Proceedings of the Ninth International Conference on Document Analysis and Recognition (ICDAR 2007)*, pp. 764–768, IEEE, Curitiba, Brazil, September 2007.
- [64] S. Dey, A. Dutta, J. I. Toledo, S. K. Ghosh, J. Lladós, and U. Pal, "Signet: Convolutional siamese network for writer independent offline signature verification," 2017, <http://arXiv:170702131>.
- [65] A. N. Azmi, D. Nasien, and F. S. Omar, "Biometric signature verification system based on freeman chain code and k-nearest neighbor," *Multimedia Tools and Applications*, vol. 76, no. 14, pp. 15341–15355, 2017.
- [66] M. B. Yilmaz and B. Yanıkoğlu, "Score level fusion of classifiers in off-line signature verification," *Information Fusion*, vol. 32, pp. 109–119, 2016.
- [67] A. Soleimani, B. N. Araabi, and K. Fouladi, "Deep Multitask Metric Learning for Offline Signature Verification," *Pattern Recognition Letters*, vol. 80, pp. 84–90, 2016.
- [68] R. Kumar, J. D. Sharma, and B. Chanda, "Writer-independent off-line signature verification using surroundedness feature," *Pattern Recognition Letters*, vol. 33, no. 3, pp. 301–308, 2012.
- [69] M. Manoj Kumar and N. B. Puhani, "Off-line signature verification: upper and lower envelope shape analysis using chord moments," *IET Biometrics*, vol. 3, no. 4, pp. 347–354, 2014.
- [70] Y. Guerbai, Y. Chibani, and B. Hadjadji, "The effective use of the one-class svm classifier for handwritten signature verification based on writer-independent parameters," *Pattern Recognition*, vol. 48, no. 1, pp. 103–113, 2015.